

Investigations on nano-iron oxides properties used for different industrial applications

E. MATEI*, A. M. PREDESCU, A. PREDESCU, E. VASILE^a, C. PREDESCU

Politehnica University of Bucharest, Material Science and Engineering Faculty, 313 Splaiul Independentei, Bucharest, Romania

^a*METAV CD, 31 C.A. Rosetti Street, Bucharest, Romania*

The paper refers at synthesis preparation of some iron oxides useful in different industrial applications, with high capacities of adsorption for different metal ions from wastewaters. The synthesis method was partial reduction coprecipitation for Fe₃O₄ nanoparticles, followed by aeration of acidified magnetite nanoparticles for obtaining the γ-Fe₂O₃ nanoparticles, and also a mechanical alloying in order to obtain a nanoscale compound, copper ferrite (CuFe₂O₄). In order to validate the obtained compounds the investigation methods were scanning electron microscopy (SEM), transmission electron microscopy (TEM), energy dispersive X-ray spectrometry (EDX) and X-ray diffraction (XRD) techniques. The stability of the nanomaterials, after 24 hours, was tested and measured with atomic absorption spectrometry (AAS).

(Received February 23, 2011; accepted March 16, 2011)

Keywords: Nanoparticle, Magnetite, Maghemite, Copper ferrite, EDX, SEM, XRD, TEM

1. Introduction

Nano-iron oxides, such as magnetite (Fe₃O₄) and maghemite (γ-Fe₂O₃), and also different ferrite compounds are known as materials used in different biological and industrial application. These materials have unique magnetic and electronic properties.

Due their chemical stability, biocompatibility and heating ability, ferrofluids of maghemite nanoparticles can be used for ferrofluids hyperthermia in tumor treatment [1].

Also, due the development in nano technology, nanoscale iron oxides have became a raw material for treating the waste waters and soils, accelerating the coagulation of sewage, removing radionuclides, adsorbing organic dyes and cleaning up the contaminated soils [2].

There are many types of nanomaterials with these characteristics, but magnetic iron oxide nanoparticles are an efficient adsorbent, which couples magnetic separation with ionic exchange capacity for removal of heavy metals pollutants [3].

The physical properties of the magnetic nanomaterials are depended on the particle size, being known that materials with nanometer-size particles (3-10 nm in diameter) exhibit novel electronic, optical, magnetic, chemical and bio-medical properties [4].

The size of the Fe₃O₄ nanoparticles is strongly dependent on the pH and the ionic strength of the precipitation medium. At a fixed ionic strength, the particle size decreases with the increasing of the pH.

At a fixed pH value, the size decreases with increasing of the ionic strength.

Above a critical pH, dependent on the ionic strength, no secondary growth takes place under aging in the pH and ionic strength conditions [5].

All information have been quantitatively expressed by applying the thermodynamic laws and the results showed that the size of the Fe₃O₄ particles can be controlled and stabilized at nanometric scale by adjusting the precipitation conditions [5].

In this paper the preparation and characterization of magnetite (Fe₃O₄), maghemite (γ-Fe₂O₃) and copper ferrite (CuFe₂O₄) are described.

2. Experimental

2.1. Preparation and characterization of magnetite (Fe₃O₄) nanoparticles

One of the oldest and most conventional techniques for nanoparticles synthesis is the precipitation method [6, 7, 8].

In general, the synthesis of monodispersed particles is performed under a kinetic control of the precipitation using very dilute solutions, the transitory precipitation of another phase or thermohydrolysis conditions.

This paper describes the method for preparation of spherical magnetite nanoparticles by partial reduction coprecipitation method. Sodium sulfite (Na₂SO₃) was added under magnetic stirring into ferric chloride (FeCl₃) dissolved in HCl. When the colour of the solution turned into black, ammonia solution was added under vigorous stirring. The black precipitate was immediately formed and the completely crystallization took place after 30 minutes. The method followed the same steps as the one described by Sun et al., 2004 [1].

The precipitate was washed by distilled water until the pH of the suspension reached at 7.5. The precipitate was separated with an external magnet and dried at ambient temperature under vacuum.

A part of this precipitate was used for obtaining the maghemite (γ - Fe_2O_3) nanoparticles.

The particle size and distribution were detected using a transmission electron microscope TECNAI F30 G², with linear resolution of 1 Å and punctual resolution of 1.4 Å. The X-ray energy dispersive qualitative microanalysis (EDX) was achieved by an EDAX detector with a resolution of 133eV. The samples were prepared on copper grids and covered by a thin Formvar film.

The structure of the Fe_3O_4 nanoparticles was characterized by X-ray powder diffraction, which was carried out in a SHIMADZU diffractometer with high-intensity Cu K α radiation ($\lambda = 1.54 \text{ \AA}$) with the 2θ range from 10° to 90° [9].

2.2. Preparation and characterization of maghemite (γ - Fe_2O_3) nanoparticles

In the literature, there are known various methods for preparation of γ - Fe_2O_3 , using different methods for synthesis, for example to get the γ - Fe_2O_3 nanoparticles, the Fe_3O_4 nanogel was first produced using the sol – gel method [2].

In this paper, in order to obtain maghemite (γ - Fe_2O_3) nanoparticles, a part from black precipitate of magnetite (Fe_3O_4) nanoparticles was diluted and pH value adjusted at 3.0 with HCl (0.1 N). The temperature was raised at 90°C and stirred under aeration for one hour. The color of the suspension changed into reddish-brown from black and the supernatant became clear and transparent. The precipitate was washed with distilled water and magnetically separated.

The size and morphology of the nanoparticles were analyzed by the same methods as magnetite nanoparticles, TEM and XRD.

2.3. Preparation and characterization of copper ferrite (CuFe_2O_4) nanoparticles

Most of the MeFe_2O_4 nanoparticles are synthesized using chemical precipitation method [10].

Also, the mechanical alloying represents another method for obtaining of MeFe_2O_4 nanoparticles. The alloying process is strongly dependent by chemical reactivity of the reagents, ambient conditions (aeration or inert gas), intensity and duration of the process. Due these

parameters, the final products can be homogenous amorphous phases or crystalline and amorphous phase mixtures.

In this paper, the experiments were carried out with a ball mill, using a ratio $\text{Fe}_3\text{O}_4 / \text{Cu}$ of 1/1 and 1/4, respectively. Duration of milling was five hours in ambient atmosphere.

The size and morphology of the obtained nanoparticles were investigated with TEM and XRD methods.

2.4. Effect of pH on nano-iron oxides

In order to evaluate the stability of nanoparticles under different pH values, the hydrochloric acid (HCl 0.1 N) and sodium hydroxide (NaOH 0.1N) were added into nano-iron suspensions. After stirring, the nano-iron oxides suspensions were isolated by centrifugation and then magnetically separated and the supernatant was analyzed by atomic absorption spectrometry (AAS) in order to establish the total dissolved iron content. The GBC 932 AB Plus spectrometer, with flame and spectral domain between 185 – 900 nm, was equipped with an iron hollow cathode lamp (HCL). Determinations were made at 283 nm. For concentrations under detection limit of the flame atomic absorption spectrometer (FAAS), an AVANTA Ultra Z graphite furnace atomic absorption spectrometer (GFAAS) with Zeeman effect was used, with analytical wavelength of 248.3 nm for iron, lamp current 12.5 mA, spectral bandwidth of 0.2 nm.

3. Results

3.1. Characterization of magnetite (Fe_3O_4) nanoparticles

The transmission electron microscopy through bright field (TEMBF) image from Fig. 1 (a) shows a good dispersion of spherical Fe_3O_4 nanoparticles at average diameter of around 10 nm. Also, in order to identify the plans associated with the maximum values of the magnetite nanoparticles was used as method the selected area electron diffraction (SAED) from Fig. 1 (b). The SAED image confirms the presence of Fe_3O_4 nanoparticles in the analyzed sample.

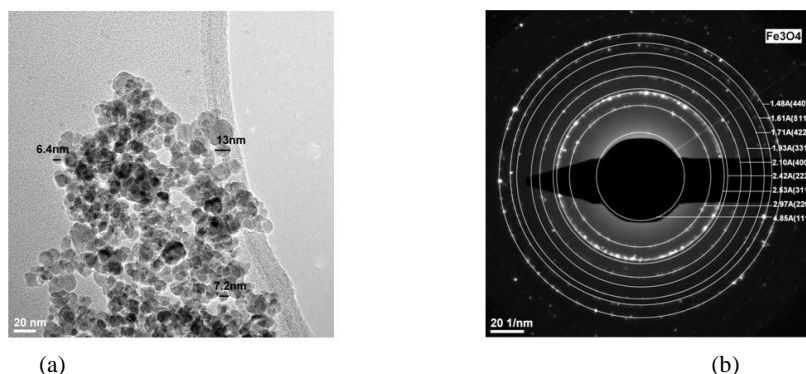


Fig. 1. (a) Electronic microscopy image through bright field transmission (TEMBF) for Fe_3O_4 nanoparticles
(b) Electron diffraction image (SAED) associated to the sample from Fig. 1 (a).

The composition of the Fe_3O_4 was confirmed by the X-ray energy dispersion (EDX) microanalysis of the analyzed area and it is presented in Fig. 2. The presence of iron and oxygen can be observed, with iron abundance higher than oxygen. Also, together with Fe and O, the copper is presented due the grids used for sample preparation. The crystalline structure of the prepared nanoparticles was verified by X-ray diffraction (XRD). All the detected diffraction peaks were indexed and the patterns are presented in the Fig. 3. The analyzed samples showed very broad diffraction lines, in accordance with their small particle size and high specific surface area. The image indicates the small dimension for synthesized magnetite, with diameters smaller than 20 nm. Combined with XRD patterns, the data indicates the inverse cubic spinel structure of Fe_3O_4 .

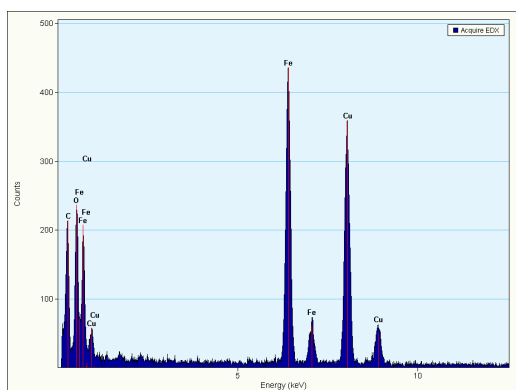
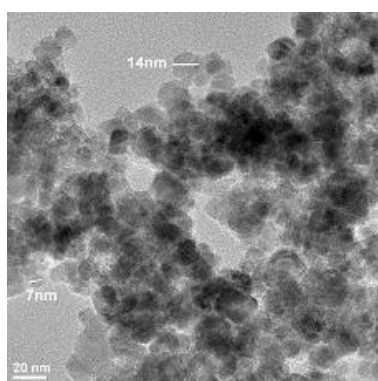
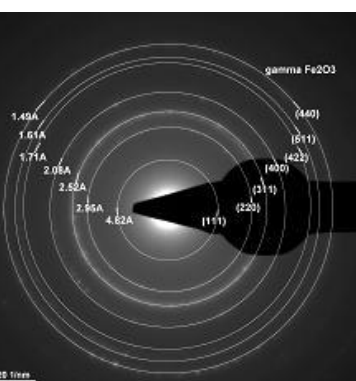


Fig. 2. EDX image for Fe_3O_4 nanoparticles.



(a)



(b)

Fig. 4. (a) TEMBF image for $\gamma\text{-Fe}_2\text{O}_3$; (b) SAED image associated to the sample from figure (a).

The analyzed product was a red-brown precipitate with a relative good dispersion and an average of diameter size of 7 nm. Also, an EDX image indicates the presence of the iron and oxygen as it is shown in the Fig. 5. The X-ray diffraction patterns of the material proved the crystalline nature. All the detected diffraction peaks that were indexed in Fig. 6 indicate that the particles correspond to maghemite. The prepared maghemite samples showed very broad diffraction lines, in accordance with their small particle size and high specific

surface area. These maghemite nanoparticles were used for adsorption studies of hexavalent chromium [12].

The difference between magnetite and maghemite appears with position and intensities of peaks. The samples analyzed had a cubic crystalline structure for the two iron oxides nanoparticles: magnetite and maghemite.

The obtained magnetite nanoparticles will be used as adsorption material for pollutants from wastewaters in the future studies.

Table 1 shows the most intense powder diffraction peaks of the Fe_3O_4 and $\gamma\text{-Fe}_2\text{O}_3$ samples. The d-spacing

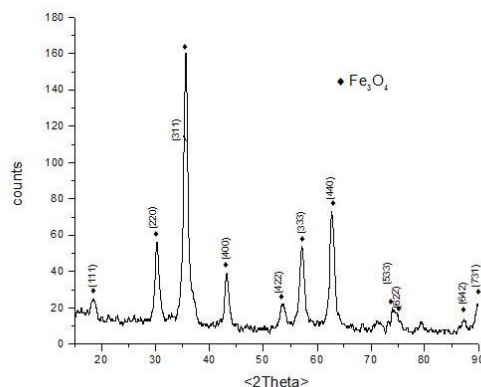


Fig. 3. XRD Pattern of Fe_3O_4 nanoparticles.

3.2. Characterization of maghemite ($\gamma\text{-Fe}_2\text{O}_3$) nanoparticles

The phase diagram of the Fe-O system shows that Fe and O forms 3 oxides: FeO (wustite), Fe_3O_4 (magnetite), Fe_2O_3 (hematite) and $\gamma\text{-Fe}_2\text{O}_3$ (maghemite). Magnetite can be found under the formula $\text{FeO}\cdot\text{Fe}_2\text{O}_3$. Through oxidation of the magnetite (Fe_3O_4), the maghemite ($\gamma\text{-Fe}_2\text{O}_3$) can be obtained. Time plays an important part in the experiment.

The obtained nanoparticles have bigger specific surface and present a higher risk of oxidation [11].

The $\gamma\text{-Fe}_2\text{O}_3$ obtained particles from aeration oxidation of acidified magnetite nanoparticles were analyzed by transmission electron microscope (TEM). The TEMBF and SAED images are shown in the Fig. 4 (a) and (b), respectively.

values (nm) calculated from the electron diffraction patterns inserted in Fig. 1 and Fig. 4 and the standard atomic spacing for Fe_3O_4 and $\gamma\text{-Fe}_2\text{O}_3$ along with respective hkl indexes from the JCPDS card (19-629) and (39-1346) respectively.

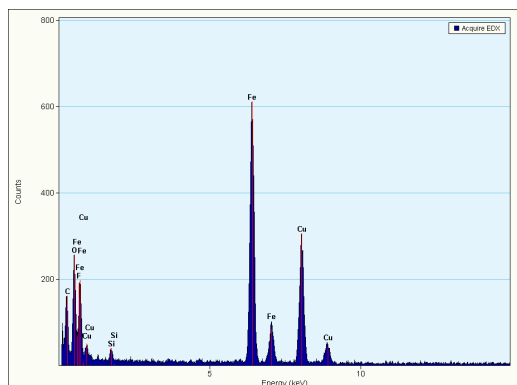


Fig. 5. The EDX spectra for $\gamma\text{-Fe}_2\text{O}_3$ nanoparticles.

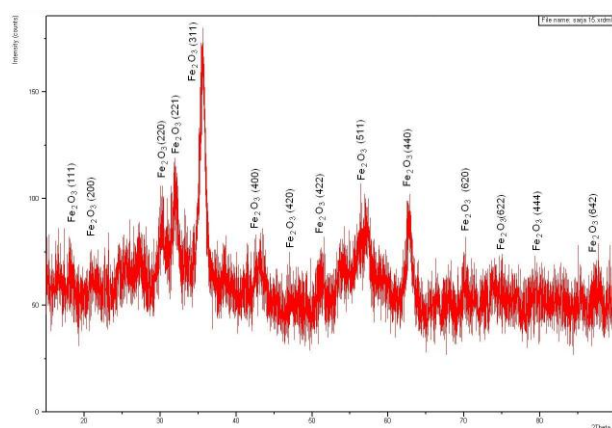


Fig. 6. XRD patterns for $\gamma\text{-Fe}_2\text{O}_3$ nanoparticles.

Table 1. The *d*-spacing values (nm) calculated from the electron diffraction patterns inserted in Fig. 1 and Fig. 4 and the standard atomic spacing for Fe_3O_4 and $\gamma\text{-Fe}_2\text{O}_3$ along with respective hkl indexes.

Ring	Calculated <i>d</i> spacing	JCPDS data for Fe_3O_4	hkl	Calculated <i>d</i> spacing	JCPDS data for $\gamma\text{-Fe}_2\text{O}_3$	hkl
1	0.486	0.483	111	0.482	0.482	111
2	0.297	0.296	220	0.295	0.295	220
3	0.253	0.252	311	0.252	0.252	311
4	0.210	0.209	400	0.208	0.208	400
5	0.193	0.192	331			
6	0.171	0.170	422	0.171	0.170	422
7	0.162	0.162	333			
8	0.161	0.161	511	0.161	0.161	511
9	0.147	0.148	440	0.149	0.148	440

3.4. Characterization of copper ferrite (CuFe_2O_4) nanoparticles

CuFe_2O_4 surface morphology analysis from TEM indicates that the agglomeration of many ultrafine particles with diameter lower than 50 nm as it can be seen in the Fig. 7. The EDX microanalysis was achieved with carbon grid in order to avoid the interference of the results. The image of EDX for CuFe_2O_4 is presented in Fig. 8.

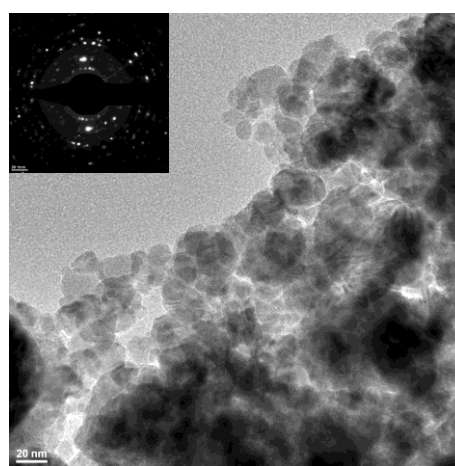


Fig. 7. TEM image for CuFe_2O_4 nanoparticles.

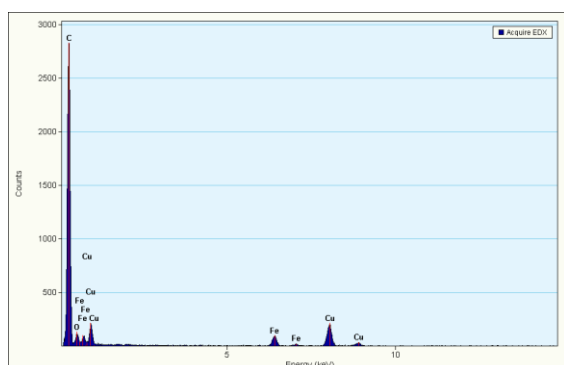


Fig. 8. EDX image for CuFe_2O_4 nanoparticles.

3.5. Effect of pH on nano-iron oxides

The total dissolved iron content was measured at pH 2.5 and 8.5. The tested nano-materials were Fe_3O_4 , $\gamma\text{-Fe}_2\text{O}_3$ and CuFe_2O_4 . The initial quantity from each nanomaterial was 0.5 g which was added at 100 mL HCl and NaOH, respectively. The contact time was between 10 and 120 minutes. After the last measurement, a new measurement was made after 24 hours. The total dissolved iron content, expressed as mg/L was measured with flame atomic absorption spectrometer (FAAS) and the results obtained for acidic conditions are shown in the Table 2.

Table 2. The FAAS measurements of the total dissolved iron concentrations, mg/L, at pH 2.5.

Time, minutes	Total dissolved iron content, mg/L, from:		
	$\gamma\text{-Fe}_2\text{O}_3$	Fe_3O_4	CuFe_2O_4
10	26.164	8.986	3.289
20	22.658	10.865	3.275
30	39.105	10.756	3.657
40	40.123	10.342	3.897
50	42.156	11.382	4.387
60	44.362	11.870	4.890
70	45.786	15.890	6.987
80	48.897	15.240	6.912
90	48.654	15.380	7.854
100	50.120	15.980	7.750
120	49.567	16.000	7.843
24 hours	52.222	19.543	8.965

It can be observed that the most total dissolved iron concentration was obtained from $\gamma\text{-Fe}_2\text{O}_3$, which had the lowest stability in acidic conditions. The concentrations of dissolved iron had increased with contact time and after 24 hours the concentration reached at 52.222 mg Fe /L. Lower concentrations can be observed in case of the Fe_3O_4 and CuFe_2O_4 .

In case of basic conditions, at pH 8.5, the results are shown in Table 3.

The total dissolved iron content, expressed as mg/L, was under detection limit of the FAAS, in case of basic conditions. The graphite furnace atomic absorption spectrometer (GFAAS) was used for measuring the trace iron from basic solutions for the three nanomaterials. It can be observed the lowest concentrations were for CuFe_2O_4 and the highest for the Fe_3O_4 .

Table 3. The GFAAS measurements of the total dissolved iron concentrations, mg/L, at pH 8.5.

Time, minutes	Total dissolved iron content, mg/L, from:		
	$\gamma\text{-Fe}_2\text{O}_3$	Fe_3O_4	CuFe_2O_4
10	0.048	0.150	0.009
20	0.000	0.150	0.005
30	0.012	0.140	0.010
40	0.015	0.134	0.010
50	0.142	0.156	0.012
60	0.100	0.176	0.075
70	0.110	0.140	0.065
80	0.090	0.120	0.073
90	0.099	0.110	0.076
100	0.130	0.130	0.069
120	0.111	0.110	0.061
24 hours	0.083	0.130	0.120

The results after 24 hours are presented in the Fig. 9, under acidic and basic conditions.

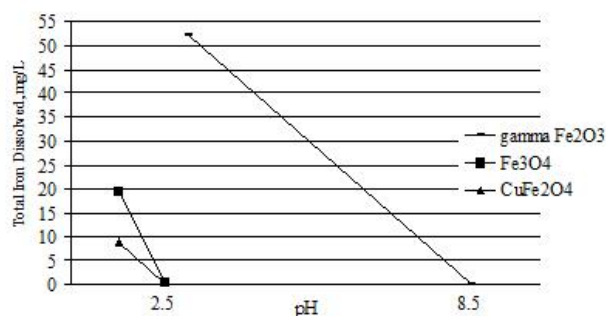


Fig. 9. The total iron dissolved concentrations (mg/L) from nanomaterials, at pH 2.5 and 8.5, after 24 hours.

4. Discussions

4.1. Characterization of Fe_3O_4 , $\gamma\text{-Fe}_2\text{O}_3$ and CuFe_2O_4 nanoparticles

From the surface morphology and size analyses by TEM, EDX and XRD, the synthesized nanomaterials have a diameter lower than 20 nm, indicating a high surface reactivity and possibility to use in different applications. The average diameter size is shown in the Table 4. Also, being magnetic nanoparticles there is an easy and cheap method for separation using a strong magnetic field. In these conditions, these nanomaterials act not only an adsorbent for removing of toxic metal ions from waste waters, but also as magnetically elements for attracting and retaining of paramagnetic nanomaterials necessary to remove from solutions [2]. Regarding the adsorption of the heavy metals from wastewaters, the adsorption of the

hexavalent chromium is known as an efficiently method for treatment of industrial effluents.

Table 4. The average diameter size for Fe_3O_4 , $\gamma-Fe_2O_3$ and $CuFe_2O_4$ nanoparticles.

Nanomaterials	Average diameter size, nm	Investigation method
Fe_3O_4	10	TEM, EDX, XRD
$\gamma-Fe_2O_3$	7	
$CuFe_2O_4$	10	

The magnetically separation of the $\gamma-Fe_2O_3$ nanoparticles, after use as adsorbent for hexavalent chromium Cr(VI) can be made in the laboratory experiments as it is shown in the Fig. 10.



Fig. 10. Magnetically separation of the $\gamma-Fe_2O_3$ used as adsorbent for removal of Cr(VI) from aqueous solutions.

The amount adsorbed is higher in comparison with others common adsorbent such as activated carbon or diatomite, according to the results from literature, namely: 11.5 mg/g for diatomite and 15.47 mg/g for activated carbon, respectively [13].

4.2. Effect of pH on nano-iron oxides

The effect of pH on synthesized nanomaterials, under acidic and basic conditions, was quantified by total dissolved iron content. The total iron concentrations at acidic pH indicated that the highest tendency of dissolution is attributed to $\gamma-Fe_2O_3$. The low but detectable level of dissolved iron concentration at basic pH is attributed to the formation of a small amount soluble (e.g., $FeOH^+$) and a higher quantities of insoluble iron hydroxides (e.g., $Fe(OH)_2$, $Fe(OH)_3$).

5. Conclusions

The magnetic nanoparticles (Fe_3O_4 , $\gamma-Fe_2O_3$ and $CuFe_2O_4$) with diameter size lower than 20 nm were synthesized using as methods:

- Partial reduction coprecipitation for Fe_3O_4 ;
- Aeration of acidified magnetite for $\gamma-Fe_2O_3$;
- Mechanical alloying for $CuFe_2O_4$.

The morphology studies confirmed the obtaining of Fe_3O_4 and $\gamma-Fe_2O_3$ nanoparticles with a good dispersion and $CuFe_2O_4$ nanoparticles agglomerated at an average size 10 nm. Also, the crystalline structure was confirmed and the microanalysis indicated the purity of the compounds.

The stability for these nanomaterials was demonstrated for basic conditions, at pH 8.5. The acidic conditions, with pH 2.5, demonstrated a high dissolution tendency, especially for $\gamma-Fe_2O_3$.

The results of this study will be applicable for testing these nanomaterials for waste water treatment, as adsorbents, being known their high surface area and reactivity.

Acknowledgements

Authors recognize financial support from the European Social Fund through POSDRU/89/1.5/S/54785 project: "Postdoctoral Program for Advanced Research in the field of nanomaterials".

References

- [1] Yong-kang Sun, Ming Ma, Yu Zhang, Ning Gu, Colloids and Surfaces A: Physicochem. Eng. Aspects **245**, 15 (2004).
- [2] Irene M.C. Lo, J. Hu, G. Chen, Nanotechnologies for Water Environment Applications, American Society of Civil Engineers (ASCE), Virginia (2009).
- [3] X. Wang, C. Zhao, P. Zhao, P. Dou, Y. Ding, P. Xu, Bioresource Technology, **100**, 2301 (2009).
- [4] D. Predoi, V. Kuncser, G. Filoti, Romanian Reports in Physics, **56**(3), 373 (2004).
- [5] J. P. Jolivet, C. Chaneac, P. Prene, L. Vayssieres, E. Tronc, J. Phys. IV France **7**, C1 573 (1997).
- [6] T. Yonezawa, S. Onoue, N. Kimizuka, Langmuir, **16**, 5218 (2000).
- [7] T. Fried, G. Shemer, G. Markovich, Adv. Mater., **13**(15), 1158 (2001).
- [8] D. H. Chen, C. H. Hsieh, J. Mater. Chem., **12**, 2412 (2002).
- [9] Andrei Predescu, Bulletin of the Polytechnic Institute of Jassy, LVI (LX), **2**, 95 (2010).
- [10] Jing Hu, Irene M.C. Lo, Guohua Chen, Separation and Purification Technology, **56**, 249 (2007).
- [11] M. A. Legodi, D. de Waal, Dyes and Pigments, **74**, 161, (2007).
- [12] Ecaterina Matei, Andra Predescu, Liana Vladutiu, Andrei Predescu, International Conference of Safe production and use of nanomaterials, P2c-1, Grenoble November 16-18, (2010).
- [13] Jing Hu, Guohua Chen, Irene M. C. Lo, Water Research, **39**, 4528 (2005).

*Corresponding author: ecaterina.matei@ecomet.pub.ro